1   TITLE
2   Photo-Controllable Phase Transition of Arylazopyrazole-Conjugated
3   Oligonucleotides
4
5   AUTHORS

6   Takuya Hidaka,[#,†] Wen Ann Wee,[#,†] Ji Hye Yum,[†] Hiroshi Sugiyama,[*,†,‡] and Soyoung Park
7   [*,†]
8   [†] Department of Chemistry, Graduate School of Science, Kyoto University, Sakyo, Kyoto 606-
9   8501, Japan
10 [‡] Institute for Integrated Cell-Material Science (WPI-iCeMS), Kyoto University, Sakyo,
11 Kyoto 606-8501, Japan.
12 [#] T. Hidaka and A. W. Wee contribute equally as first authors.
13
14 Correspondence: hs@kuchem.kyoto-u.ac.jp, oleesy@kuchem.kyoto-u.ac.jp
15
16 ABSTRACT

17   Phase transition is a promising aspect of DNA as biopolymers. Anionic DNA
18 oligonucleotides easily form complexes with cationic polypeptides such as poly-lysine, and
19 duplex formation significantly influences their complexation and resulting
20 microcompartments. In this study, phase transition of microcompartments containing DNA
21 and poly-lysine was systematically induced by modulating duplex formation of
22 arylazopyrazole-conjugated oligonucleotides with light. We demonstrated that UV irradiation
23 destabilized DNA duplex and generated isotropic coacervates, while duplex stabilization by
24 visible light irradiation caused formation of liquid crystalline coacervates. This photo-control
25 of phase transition was highly repeatable, and similar changes were observed even after ten
26 cycles of light irradiation. Our approach would provide a robust control layer to the
27 development of tailor-made microcompartments.
28
29 **Table of Contents Graphic**
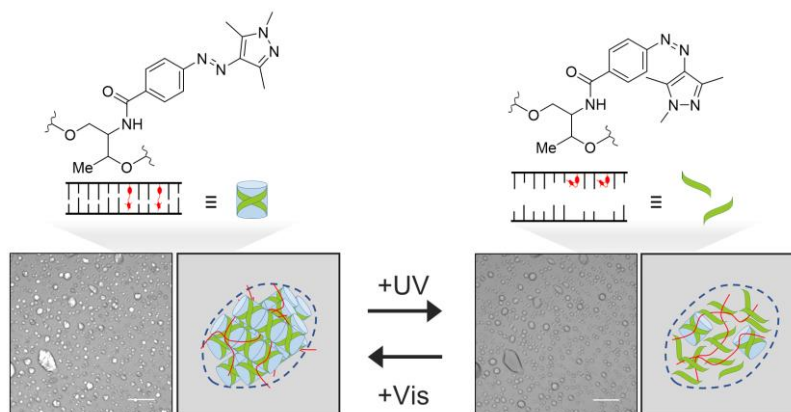
30
31

DNA is a biopolymer composed of nucleotide units containing a phosphate, a sugar and four distinct bases: A, T, G and C. The bases A and G form complementary Watson–Crick base pairs with T and C respectively through hydrogen-bonding interactions. The high specificity of the base-pairing and the formation of a duplex with a precise structure are not only effective to store and transfer genetic information, but also enable us to design a variety of structures, making DNA a powerful tool in nanotechnology and material science. For example, branched double-stranded DNA (dsDNA) structures with sticky single-stranded DNA ends are commonly used to build up two- and three-dimensional structures, and DNA origami technology clearly exemplifies the structural programmability of DNA as a platform to construct desired shapes. [1-3] Functional programmability is another advantage of DNA as a material. Although functions achievable with natural bases are limited, the applications of DNA have been expanded through artificial monomers possessing properties not present in natural bases, such as fluorescence and photo-responsivity. [4, 5] Because DNA can be synthesized by solid-phase synthesis, a number of artificial monomers can be readily introduced at any position in the strand. [6, 7] The exemplary structural and functional programmability of DNA allows us to convert DNA into a tailor-made material with the desired structures and functions via modular design. To exploit this advantage in organic syntheses, we have investigated the catalytic functions of DNA with unnatural monomer units. For example, we have incorporated a bipyridine ligand into DNA to generate DNA metalloenzymes for enantioselective hydration reactions, and devised histidine-modified oligonucleotides showing remarkable metal-binding ability and catalytic performance for DNA-based asymmetric catalysis as well as ABTS oxidation reactions.[8-10] This 'bottom-up' molecular engineering technology is useful in endowing DNA/RNA oligonucleotides with new functions such as catalysis and molecular switching.

In recent years, it has been reported that phase transition and separation play important roles in intracellular compartmentalization and biochemical reactions in living cells. Membraneless oligonucleotide and protein condensates are associated with the control of genetic information such as RNA processing. [11, 12] Phase transitions between liquid, gel, and solid, and the multi-phase coexistence endow cells with spatiotemporal control over intracellular processes. [13-15] Phase transition and separation are promising aspects of DNA as biopolymers, enabled by their ability to form multi-valent interactions between DNA/RNA nanostructures or nucleic acid binding proteins. [16-18] In addition to their biological significance, [19-21] the artificial control of microcompartment formation using DNA is attracting researchers' interest because it allows for the dynamic regulation of chemical or enzymatic reactions in the microcompartments, which is beneficial for synthetic protocell research and the sequence-specific design of artificial molecular systems. [22-24] Recently, Mann and coworkers have

reported the photo-control of droplet formation using a mixture of dsDNA and an azobenzene cation.[25] In another study, Takinoue and his group achieved the sequence-based design of micrometer-sized DNA droplets with Y-shaped DNA nanostructures possessing sticky ends.[26] Interestingly, anionic DNA oligonucleotides easily form complexes with cationic polypeptides like poly-lysine to generate phase-separated compartments.[27] The flexibility and charge density of DNA significantly influence their complexation and the resulting microcompartments: i.e., ssDNA which has high flexibility and low charge density forms liquid coacervates, while rigid and highly charged dsDNA tends to form solid precipitates or liquid-crystal coacervates. [18, 28-30] Leveraging on the pioneering studies by Asanuma and colleagues, which have propelled the photocontrol of DNA duplex formation by azobenzene isomerization to a powerful tool in biotechnology and DNA nanotechnology,[5, 31, 32] we were motivated to expand this technology to the photo-regulation of microcompartments.

We hypothesized that we could control phase transition through the photo-regulation of DNA duplex formation. DNA oligonucleotides bearing arylazopyrazoles (AAPs) as light-responsive moieties (AAP-DNA) are regarded as versatile photoswitches as they enable the control of the hybridization and dissociation of DNA duplexes depending on the irradiated wavelengths.[33] Compared with azobenzene, AAP shows rapid and high yield in trans-to-cis isomerization under UV irradiation.[34] In addition, cis-to-trans isomerization can be achieved by photoirradiation at a long wavelength (> 520 nm).[33, 34] Based on these significant features of AAP, herein, we demonstrate a photo-regulation system for the phase transition of microcompartments with AAP-conjugated oligonucleotides.

The schematic illustration of our hypothesis is shown in Fig. 1. In trans state, AAP-DNA can form a duplex with its complementary strand and in the presence of poly-lysine, rigid duplex DNA is expected to form liquid crystal coacervates (Fig. 1, left). When the duplex is dissociated and flexible ssDNA strands are released after UV irradiation and subsequent cis isomerization, the microcompartments would be converted into isotropic coacervates (Fig. 1, right). Visible light irradiation, resulting in the reversion of AAP to its trans state, would change them back to liquid crystal coacervates.

To examine our hypothesis, DNA oligonucleotides with and without two AAP moieties (AAP-ODN1 and ODN1, respectively) and their complementary strand (ODN2) were prepared (Table 1). Because AAP moieties were additionally introduced to ODN1, AAP-ODN1 has two extra negative charges compared to ODN1 (Fig. S1).
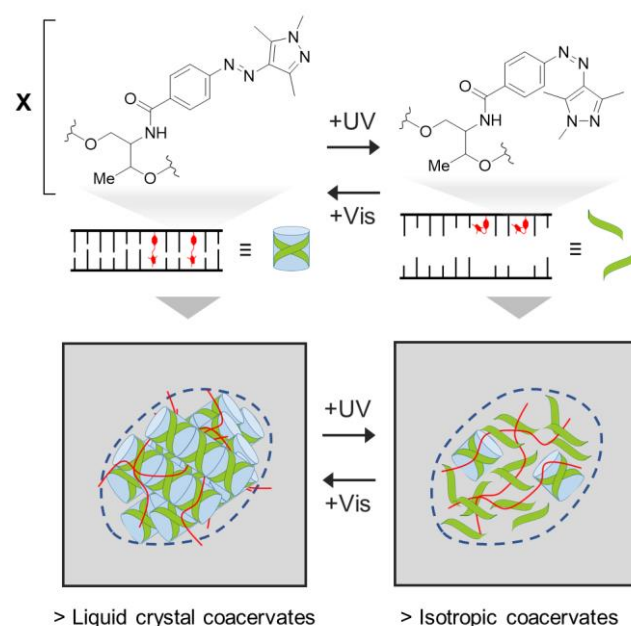
1

2 **Fig. 1   Schematic illustration of photocontrol of phase transition.**

3

4 **Table 1. Sequence of DNA used in this study (X = AAP).**

5 [a] The chemical structure of AAP-ODN1 is shown in Fig. S1.

Name	Sequence (5'>3')
AAP-ODN1[a]	TG**X**AA**X**CTAACG
ODN1	TGAACTAACG
ODN2	CGTTAGTTCA
ODN2'	CGTTAGAAGT

6

7 To confirm photo-switchable AAP isomerization and DNA duplex formation, we measured

8 the absorbance spectra and melting temperature (T_m) of AAP-ODN1/ODN2 (Fig. 2). In the

9 absorbance spectra, we observed two peaks before UV irradiation, one was a typical peak of

10 DNA around 260 nm and the other peak was found around 360 nm, which corresponds to the

11 absorption of AAP in the trans form (Fig. 2A).[33] The latter peak was reduced after UV

12 irradiation and was recovered by visible light irradiation, indicating that isomerization of AAP

13 can be controlled by light irradiation in a wavelength-dependent manner. Consistently, while

14 the T_m values of AAP-ODN1/ODN2 before light irradiation and after sequential UV and

15 visible light irradiation were calculated to be 31.1°C (±0.3°C) and 30.1°C (±0.0°C),

16 respectively (each S.D. is indicated in parentheses, n = 2), a clear inflection in absorbance

17 was not observed after the UV irradiation suggesting that the stability of AAP-ODN1/ODN2

18 duplex is also photo-controllable (Fig. 2B). An increase in absorbance at 360 nm of UV-

4

1 irradiated AAP-ODN1/ODN2 during the melting curve experiments indicated that cis-to-
2 trans isomerization occurs at a high temperature (Fig. S2A). To reveal the hybridization state
3 of AAP-ODN1/ODN2, melting curves of AAP-ODN1 with ODN2' —which can form a 6 bp
4 duplex with the partial sequence in AAP-ODN1 not containing AAP moieties—and ODN1—
5 which does not form a duplex with AAP-ODN1—were also obtained (Fig. S2B and C).
6 Melting curves of AAP-ODN1/ODN2' did not show any inflection points even without UV
7 irradiation and only a small increase by around 0.01 was observed from 10°C to 20°C, which
8 indicates that hybridization of the AAP-containing region is important for photocontrol of
9 duplex formation, (Fig. S2B). Because this increase became even smaller in AAP-
10 ODN1/ODN1, it is expected that the 6 bp partial duplex is formed at low temperatures below
11 20°C (Fig. S2C).
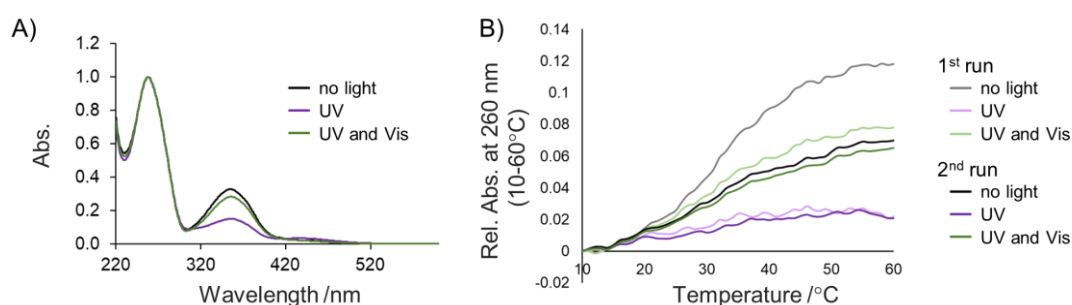
12

13 Fig. 2   (A) Absorbance spectra and (B) melting curves of the AAP-ODN1/ODN2 with and
14 without light irradiation. Samples were subjected to UV (365 nm) irradiation or sequential UV
15 and visible light (520 nm) irradiation. The melting curves are shifted to start from 0 at 10°C.

16 Next, we performed polarized light microscopy to investigate the effect of light irradiation
17 on microcompartments formed in the AAP-DNA and poly-lysine mixture. AAP-ODN1 and
18 ODN2 (0.25 mM each corresponding to phosphate concentrations of 2.75 mM and 2.25 mM
19 respectively) were mixed with poly-lysine (amine concentration of 5 mM) in aqueous buffer
20 supplemented with 100 mM of NaCl.[35] It was confirmed that microcompartments containing
21 DNA and poly-lysine were formed by using fluorescently labeled ODN2 and poly-lysine (Fig.
22 S3). The samples were subjected to sequential light irradiation and each sample was imaged
23 with a laser scanning microscope attached with a polarizer (Fig. 3A and Fig. S4). While
24 precipitate-like birefringent structures were observed before light irradiation, UV (340-390
25 nm) irradiation converted them into isotropic coacervates. When visible light (530-550 nm)
26 was irradiated, birefringent phases appeared again in microcompartments. Based on the
27 previous study on dsDNA–poly-lysine coacervates, the birefringent phases are expected to be
28 liquid crystalline mesophases formed through end-to-end stacking interaction of the DNA
29 duplexes.[18] This photo-control of phase transition was highly repeatable, and similar changes
30 were observed even after ten cycles of light irradiation. Because no microcompartments were

formed at a higher concentration of NaCl (500 mM), electrostatic interactions between DNA and poly-lysine are likely to play an important role in coacervation (Fig. S5). Together with the result of the T_m assay, this indicates that photocontrol of DNA duplex formation can be expanded to the control of the phase of microcompartments. Because AAP-DNA retains its sequence information, such photo-responsivity was expected to be absent with non-complementary DNA strands. To investigate this, AAP-ODN1 was mixed with ODN1, which does not form a duplex with AAP-ODN1 as it has the same sequence as AAP-ODN1 (Fig. 3B). As expected, liquid microcompartments were formed and phase transition by light irradiation was not observed. This result shows the advantage of this system: we can selectively program the DNA pair to be subjected to photo-regulation. The microcompartments also showed a prompt response to UV (365 nm) and visible light (473 nm) irradiation in time-lapse imaging (Fig. 4, Movie S1 and S2).
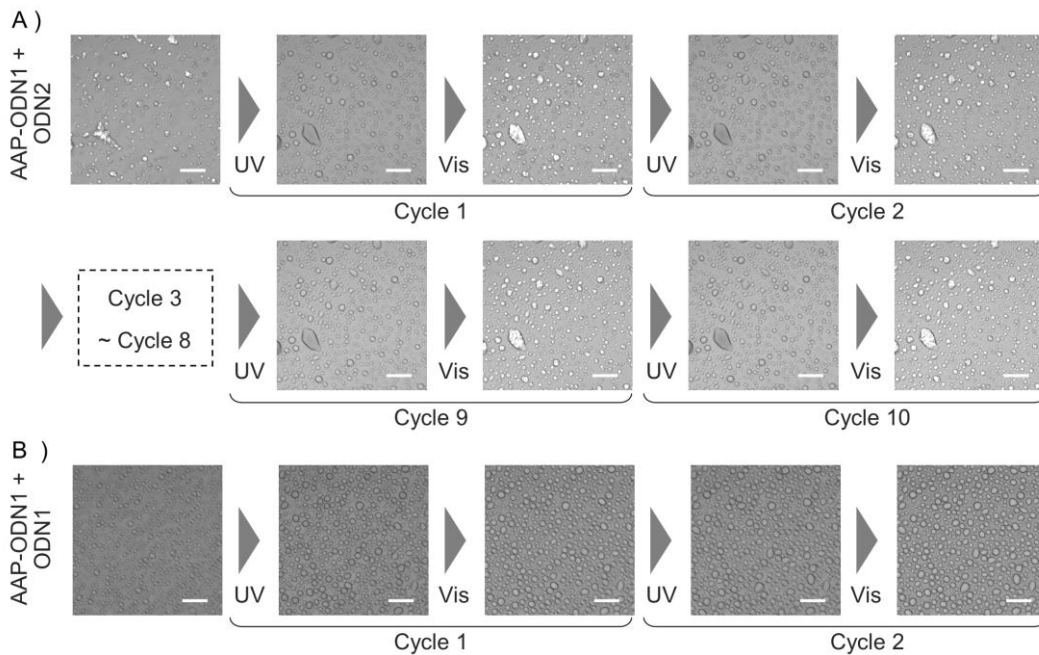
Fig. 3 Polarized light microscopy images of microcompartments during repeated UV (340-390 nm) and visible light (530-550 nm) irradiation containing (A) AAP-ODN1/ODN2 and (B) AAP-ODN1/ODN1. Scale bars are 20 μm. All images of the AAP-ODN1/ODN2 sample during the experiment are shown in Fig. S4.
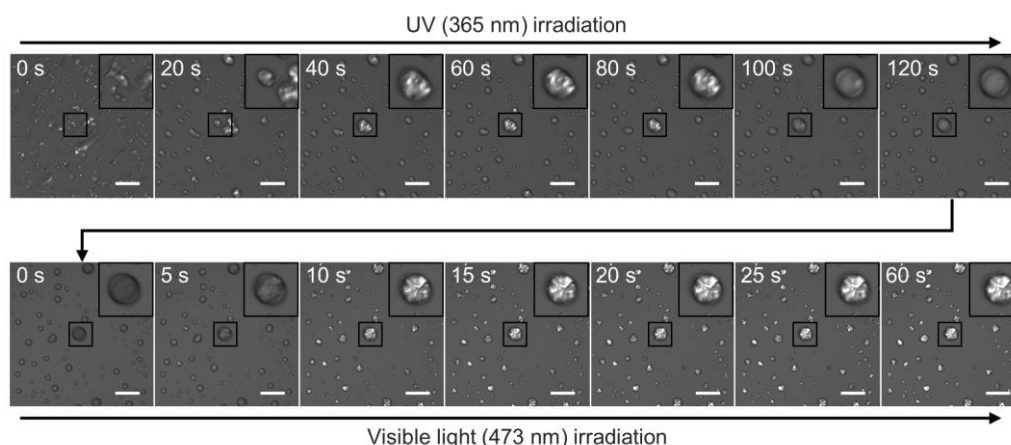
Fig. 4 Time-lapse images of microcompartments during the first UV (365 nm) and visible light (473 nm) irradiation containing AAP-ODN1/ODN2. Scale bars are 20 μm.

In conclusion, we achieved photo-control of phase transition of microcompartments formed with DNA and poly-lysine by modulating duplex formation of arylazopyrazole-conjugated oligonucleotides. The use of light to control the dynamics and functions of biomolecules is very attractive because it can be directed in terms of time and space. The present study demonstrated the conceptual simplicity and systematic tunability of arylazopyrazole-conjugated oligonucleotides for the manipulation of the nucleic acid scaffold with light. This photo-responsive phase transition would guide us toward the development of useful approaches for the regulation of molecular machinery.

ASSOCIATED CONTENT

Supporting Information

       Material and methods, HPLC and MALDI-TOF MS data, melting curves of AAP-ODN1/ODN2, AAP-ODN1/ODN2' and AAP-ODN1/ODN1, microscopic images of microcompartments (PDF)

       Movies of time-lapse images during UV and visible light irradiation. (MP4)

AUTHOR INFORMATION

Corresponding Authors

Soyoung Park – Department of Chemistry, Graduate School of Science, Kyoto University, Sakyo, Kyoto 606-8501, Japan; Email: oleesy@kuchem.kyoto-u.ac.jp

Hiroshi Sugiyama – Department of Chemistry, Graduate School of Science, Kyoto University, Sakyo, Kyoto 606-8501, Japan; Institute for Integrated Cell-Material Science (WPI-iCeMS), Kyoto University, Sakyo, Kyoto 606-8501, Japan; Email: hs@kuchem.kyoto-u.ac.jp

9

10 **DECLARATION OF INTETERESTS**

11 The authors declare no competing interests.

REFERENCES

1. Seeman, N. C., Nucleic Acid Junctions and Lattices. (1982) *J. Theor. Biol. 99*, 237-247.

2. Chen, J., Seeman, N. C. (1991) Synthesis from DNA of a molecule with the connectivity of a cube. *Nature 350*, 631-633.

3. Rothemund, P. W. (2006) Folding DNA to create nanoscale shapes and patterns. *Nature 440*, 297-302.

4. Xu, W., Chan, K. M., Kool, E. T. (2017) Fluorescent nucleobases as tools for studying DNA and RNA. *Nat. Chem. 9*, 1043-1055.

5. Kamiya, Y., Asanuma, H. (2014) Light-driven DNA nanomachine with a photoresponsive molecular engine. *Acc. Chem. Res. 47*, 1663-1672.

6. Park, S., Zheng, L., Kumakiri, S., Sakashita, S., Otomo, H., Ikehata, K., Sugiyama, H. (2014) Development of DNA-Based Hybrid Catalysts through Direct Ligand Incorporation: Toward Understanding of DNA-Based Asymmetric Catalysis. *ACS Catalysis 4*, 4070-4073.

7. Yum, J. H., Sugiyama, H., Park, S. (2020) Modular quadruplex-duplex hybrids as biomolecular scaffolds for asymmetric Michael addition reactions. *Org. Biomol. Chem. 18*, 6812-6817.

8. Park, S., Okamura, I., Sakashita, S., Yum, J. H., Acharya, C., Gao, L., Sugiyama, H. (2015) Development of DNA Metalloenzymes Using a Rational Design Approach and Application in the Asymmetric Diels–Alder Reaction. *ACS Catalysis 5*, 4708-4712.

9. Yum, J. H., Park, S., Hiraga, R., Okamura, I., Notsu, S., Sugiyama, H. (2019) Modular DNA-based hybrid catalysts as a toolbox for enantioselective hydration of alpha,beta-unsaturated ketones. *Org. Biomol. Chem. 17*, 2548-2553.

10. Park, S., Matsui, H., Fukumoto, K., Yum, J. H., Sugiyama, H. (2020) Histidine-conjugated DNA as a biomolecular depot for metal ions. *RSC Advances 10*, 9717-9722.

11. Laflamme, G., Mekhail, K. (2020) Biomolecular condensates as arbiters of biochemical reactions inside the nucleus. *Commun. Biol. 3*, 773.

12. Roden, C., Gladfelter, A. S. (2021) RNA contributions to the form and function of biomolecular condensates. *Nat. Rev. Mol. Cell. Biol. 22*, 183-195.

13. Patel, A., Lee, H. O., Jawerth, L., Maharana, S., Jahnel, M., Hein, M. Y., Stoynov, S., Mahamid, J., Saha, S., Franzmann, T. M., et al. (2015) A Liquid-to-Solid Phase Transition of the ALS Protein FUS Accelerated by Disease Mutation. *Cell 162*, 1066-1077.

14. Langdon, E. M., Qiu, Y., Niaki, A. G., McLaughlin, G. A., Weidmann, C. A., Gerbich, T. M., Smith, J. A., Crutchley, J. M., Termini, C. M., Weeks, K. M., et al. (2018) mRNA structure determines specificity of a polyQ-driven phase separation. *Science 360*, 922-927.

15. Lafontaine, D. L. J., Riback, J. A., Bascetin, R., Brangwynne, C. P. (2021) The nucleolus as a multiphase liquid condensate. *Nat. Rev. Mol. Cell. Biol. 22*, 165-182.

16. Kohata, K., Miyoshi, D. (2020) RNA phase separation-mediated direction of molecular

trafficking under conditions of molecular crowding. *Biophys. Rev. 12*, 669-676.

17. Ryu J. K., Bouchoux C., Liu H. W., Kim E., Minamino M., de Groot R., Katan A. J., Bonato A., Marenduzzo D., Michieletto D., et al. (2021) Bridging-induced phase separation induced by cohesin SMC protein complexes. *Sci. Adv. 7*, eabe5905.

18. Fraccia, T. P., Jia, T. Z. (2020) Liquid Crystal Coacervates Composed of Short Double-Stranded DNA and Cationic Peptides. *ACS Nano 14*, 15071-15082.

19. Hnisz, D., Shrinivas, K., Young, R. A., Chakraborty, A. K., Sharp, P. A. (2017) A Phase Separation Model for Transcriptional Control. *Cell 169*, 13-23.

20. Chong, S., Dugast-Darzacq, C., Liu, Z., Dong, P., Dailey, G. M., Cattoglio, C., Heckert, A., Banala, S., Lavis, L., Darzacq, X., et al. (2018) Imaging dynamic and selective low-complexity domain interactions that control gene transcription. *Science 361*, eaar2555.

21. Sanulli, S., Trnka, M. J., Dharmarajan, V., Tibble, R. W., Pascal, B. D., Burlingame, A. L., Griffin, P. R., Gross, J. D., Narlikar, G. J. (2019) HP1 reshapes nucleosome core to promote phase separation of heterochromatin. *Nature 575*, 390-394.

22. Fraccia, T. P., Smith, G. P., Zanchetta, G., Paraboschi, E., Yi, Y., Walba, D. M., Dieci, G., Clark, N. A., Bellini, T. (2015) Abiotic ligation of DNA oligomers templated by their liquid crystal ordering. *Nat. Commun. 6*, 6424.

23. Todisco, M., Fraccia, T. P., Smith, G. P., Corno, A., Bethge, L., Klussmann, S., Paraboschi, E. M., Asselta, R., Colombo, D., Zanchetta, G., et al. (2018) Nonenzymatic Polymerization into Long Linear RNA Templated by Liquid Crystal Self-Assembly. *ACS Nano 12*, 9750-9762.

24. Poudyal, R. R., Guth-Metzler, R. M., Veenis, A. J., Frankel, E. A., Keating, C. D., Bevilacqua, P. C. (2019) Template-directed RNA polymerization and enhanced ribozyme catalysis inside membraneless compartments formed by coacervates. *Nat. Commun. 10*, 490.

25. Martin, N., Tian, L., Spencer, D., Coutable-Pennarun, A., Anderson, J. L. R., Mann, S. (2019) Photoswitchable Phase Separation and Oligonucleotide Trafficking in DNA Coacervate Microdroplets. *Angew. Chem. Int. Ed. 58*, 14594-14598.

26. Sato, Y., Sakamoto, T., Takinoue, M. (2020) Sequence-based engineering of dynamic functions of micrometer-sized DNA droplets. *Sci. Adv. 6*, eaba3471.

27. Miyoshi, D., Ueda, Y. M., Shimada, N., Nakano, S., Sugimoto, N., Maruyama, A. (2014) Drastic stabilization of parallel DNA hybridizations by a polylysine comb-type copolymer with hydrophilic graft chain. *ChemMedChem 9*, 2156-63.

28. Nakata, M., Zanchetta, G., Chapman, B. D., Jones, C. D., Cross, J. O., Pindak, R., Bellini, T., Clark, N. A. (2007) End-to-End Stacking and Liquid Crystal Condensation of 6–to 20–Base Pair DNA Duplexes. *Science 318*, 1276-1279.

29. Vieregg, J. R., Lueckheide, M., Marciel, A. B., Leon, L., Bologna, A. J., Rivera, J. R., Tirrell, M. V. (2018) Oligonucleotide-Peptide Complexes: Phase Control by Hybridization. *J. Am. Chem.*

Soc. 140, 1632-1638.

30. Shakya, A., King, J. T. (2018) DNA Local-Flexibility-Dependent Assembly of Phase-Separated Liquid Droplets. *Biophys. J. 115*, 1840-1847.

31. Asanuma, H., Liang, X., Nishioka, H., Matsunaga, D., Liu, M., Komiyama, M. (2007) Synthesis of azobenzene-tethered DNA for reversible photo-regulation of DNA functions: hybridization and transcription. *Nat. Protoc. 2*, 203-12.

32. Wu, L., He, Y., Tang, X. (2015) Photoregulating RNA digestion using azobenzene linked dumbbell antisense oligodeoxynucleotides. *Bioconjug. Chem. 26*, 1070-9.

33. Adam, V., Prusty, D. K., Centola, M., Skugor, M., Hannam, J. S., Valero, J., Klockner, B., Famulok, M. (2018) Expanding the Toolbox of Photoswitches for DNA Nanotechnology Using Arylazopyrazoles. *Chem. Eur. J. 24*, 1062-1066.

34. Weston, C. E., Richardson, R. D., Haycock, P. R., White, A. J., Fuchter, M. J. (2014) Arylazopyrazoles: azoheteroarene photoswitches offering quantitative isomerization and long thermal half-lives. *J. Am. Chem. Soc. 136*, 11878-81.

35. Zanchetta, G., Nakata, M., Buscaglia, M., Bellini, T., Clark, N. A. (2008) Phase separation and liquid crystallization of complementary sequences in mixtures of nanoDNA oligomers. *Proc. Natl. Acad. Sci. U.S.A. 105*, 1111-1117.

Photo-Controllable Phase Transition of Arylazopyrazole-Conjugated Oligonucleotides

Takuya Hidaka,[#,†] Wen Ann Wee,[#,†] Ji Hye Yum,[†] Hiroshi Sugiyama,[*,†,‡] and Soyoung Park[*,†]

[†] Department of Chemistry, Graduate School of Science, Kyoto University, Sakyo, Kyoto 606-8501, Japan

[‡] Institute for Integrated Cell-Material Science (WPI-iCeMS), Kyoto University, Sakyo, Kyoto 606-8501, Japan.

[#] T. Hidaka and A. W. Wee contribute equally as first authors.

Correspondence: hs@kuchem.kyoto-u.ac.jp, oleesy@kuchem.kyoto-u.ac.jp

Contents

Method and Materials

Materials

Phosphoramidochloridous acid was received from Wako Chemicals and used without further purification. Poly-L-lysine (pLys) hydrobromide (MW 30,000-70,000) was purchased from Sigma-Aldrich Chemicals Co. and used as received. *N*, *N*-diisopropylethylamine (DIPEA) was purchased from Nacalai and used as received. Nuclease-free water was purchased from Life Technologies Corporation and used as received. All other chemicals and solvents were purchased from Sigma-Aldrich Chemicals Co., Wako Pure Chemical Ind. Ltd., TCI, or Kanto Chemical Co. Inc. and used without further purification. Glass slides (24×60 mm, thickness 0.13-0.17 mm) and coverslips (18×18 mm, thickness 0.12-0.17 mm) were purchased from Matsunami Glass and used as received.

Glen-Pak™ DNA and RNA cartridges columns were purchased at Glen Research. ODN1, ODN2, and ODN2' were obtained from Sigma Genosys. Water was deionized (specific resistance of ~ 18.2 MW cm at 25 °C) by a Milli-Q system (Millipore Corp.). All reactions were carried out under an argon atmosphere unless otherwise stated.

Oligonucleotide Synthesis

AAP-containing oligonucleotide, AAP-ODN1 were synthesized on solid supports using DMTr-protected AAP phosphoramidite and commercially available $O^{5'}$-dimethoxytrityl-2'-deoxyribonucleoside $O^{3'}$-phosphoramidites. The detailed synthetic route and characterization data for DMTr-protected AAP were reported by Adam, V. and co-workers.[1] DMTr-protected AAP phosphoramidite was prepared by dropwise addition of DIPEA at 0 °C to a solution of DMTr-protected AAP in CH$_2$Cl$_2$ followed by stirring at 0 °C for 10 min. Phosphoramidochloridous acid was subsequently added and the mixture was stirred for a further 10 min at 0 °C before warming to room temperature and stirring for another 1 h. After removal of the solvent, the residue was dissolved in MeCN and used immediately without purification for solid-phase DNA synthesis. Solid-phase oligonucleotide synthesis was performed on an ABI DNA synthesizer (Applied Biosystem, Foster City, CA). The modified phosphoramidite was chemically synthesized as described above and without purification incorporated into oligonucleotide through coupling reaction for 10 minutes. The coupling yields of AAP phosphoramidite were around 10 % less than the ones obtained with standard phosphoramidite building blocks.

Cleavage from the solid support and deprotection were accomplished with 50:50 of MeNH$_2$ in 40 wt. % in water and NH$_3$ in 28 wt. % in water at RT for 15 min and then at 65 °C for 15 min. The synthesized oligonucleotides were eluted from Glen-Pak™ DNA purification cartridges and purification steps were performed as per procedure. The final elution was subjected to normal-phase HPLC purification (2 % to 30 % ACN in 50 mM TEAA (pH 7.0) buffer, flow rate of 3.0 mL/min). After purification by HPLC, the products were confirmed by MALDI-TOF MS using a Bruker microflex-KSII (Bruker Corporation, Billerica, MA) and the purity was checked by HPLC (Table S1 and S2). DNA concentrations were determined using NanoDrop ND-1000 (NanoDrop Technologies, Wilmington, DE).

For HPLC analysis, COSMOSIL 5C$_{18}$ AR-II (Nacalai Tesque, Inc., Kyoto, 150 × 4.6 mm id), a linear gradient of 2 % to 30 % acetonitrile (in 50 mM TEAA (pH 7.0) buffer) over 30 min at a flow rate of 1.0 mL/min and detection at 254 nm were used.

Absorbance spectra measurement

The sample was prepared in a total volume of 110 μL containing 2.5 μM AAP-ODN1, 2.5 μM ODN2 and 100 mM NaCl. After annealing of the sample by heating at 95 °C for 5 min followed by slow cooling to room temperature, the sample was alternatively irradiated with UV light (365 nm, 100% intensity) by a ZUV-C30H system equipped with a ZUV-H30M head unit (Omron, UV-LED with maximum output of 500 mW) for 10 min and green light (520 nm) by HM-3 monochromatic light source equipped with a 300 W xenon lamp (JASCO) for 10 min at room temperature. After each irradiation, UV-vis absorbance spectra were measured from 220 nm to 600 nm at 20°C on a JASCO V-750 spectrophotometer equipped with a JASCO PAC-743R thermocontrolled cell changer and a JASCO CTU-100 thermocirculator.

Melting temperature (T_m) analysis

The buffer for T_m analysis was an aqueous solution of 100 mM sodium chloride and 10 mM sodium cacodylate at pH 7.0. The concentration of each DNA strand was 3 μM. Before the analyses, the samples were annealed from 65°C to 5°C at 1.0°C/min. The annealed samples were subjected to UV (365 nm, 100% intensity) irradiation with a ZUV-C30H system equipped with a ZUV-H30M head unit (Omron, UV-LED with maximum output of 500 mW) and green light (520 nm) irradiation with HM-3 monochromatic light source equipped with a 300 W xenon lamp (JASCO) for 15 min on ice. After light irradiation, absorbance at 260 nm was recorded from 5°C to 65°C at a rate of 1.0°C/min using a spectrophotometer V-650 (JASCO) with a thermocontrolled PAC-743R cell changer (JASCO) and a thermal circulator F25-ED (Julabo). The T_m values were calculated with Spectra Manager software (JASCO).

Polarized Light Microscopy Observation

All microscope slides and coverslips were treated with BSA for surface passivation. They were sonicated in acetone, methanol, and isopropanol for 5 min each and dried in an oven (60°C) for at least 1 h. 3.5% BSA solution was put on glass slides and coverslips and incubated for 15 min. After the BSA treatment, they were rinsed with deionized water and air-dried. Samples containing the oligonucleotides in NaCl solution were annealed by heating at 95°C followed by slow cooling to room temperature over three hours before the addition of pLys in pH 7.5 TE buffer (final amine concentration of 5 mM; final concentration of 0.25 mM for each oligonucleotide, final NaCl concentration of 100 mM). The annealed DNA solution was mixed with pLys on a microscope slide at room temperature and observation was started within 5 min after the addition of pLys. To minimize evaporation of the sample, edges of the coverslip were sealed with vacuum grease and an aluminum spacer was included to ensure constant sample thickness.

Samples were imaged with Olympus Laser Scanning Biological Microscope FV1200 IX83 attached with a polarizer with its associated FV10-ASW 4.2 software. For photoswitching experiments, the in-built

Olympus U-HGLGPS equipped with a 130 W mercury vapor short arc lamp and FUW (340-390 nm, 100% intensity) or FGW (530-550 nm, 100% intensity) fluorescent mirror unit was used for UV or green light irradiation, respectively. The light irradiation was performed at room temperature for 2 min. For the time-lapse imaging, a ZUV-C30H system equipped with a ZUV-H30M head unit (Omron, UV-LED with maximum output of 500 mW) was used as a UV light source (365 nm, 10% intensity) and phase-contrast images were obtained with 559 nm laser (15 mW) at the intensity of 1.0%. The following time-lapse images during visible light irradiation were obtained by 473 nm laser (15 mW) scanning at the intensity of 0.1% without UV irradiation.

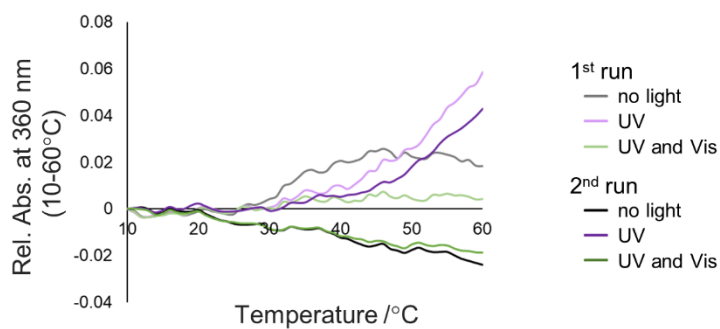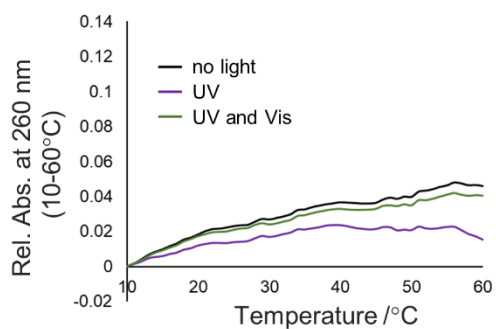Table S1. Analytical HPLC profile of synthesized oligonucleotides
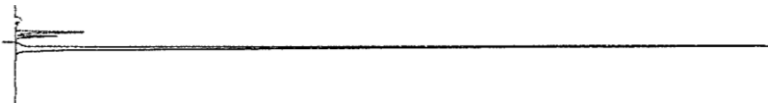
Name	HPLC Profile
AAP-ODN1	18.092 20 —

Table S2. MALDI-TOF-MS data of oligonucleotides

Name	Calcd.	Found
AAP-ODN1	3848.836	3851.43

Fig S1. Chemical structure of AAP-ODN1.

A) AAP-ODN1 + ODN2

B) AAP-ODN1 + ODN2'

C) AAP-ODN1 + ODN1
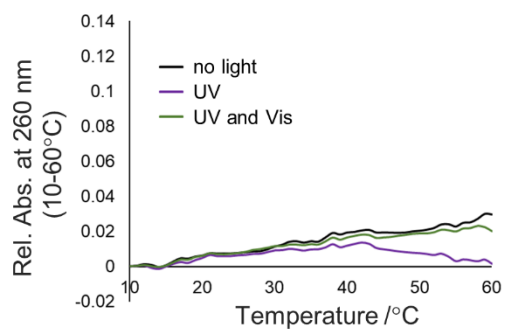
Fig S2. (A) Absorbance of AAP-ODN1/ODN2 at 360 nm during the DNA melting experiments. (B, C) Melting curves of AAP-ODN1/ODN2' (B) and AAP-ODN1/ODN1 (C). The melting curves are shifted to start from 0 at 10°C.
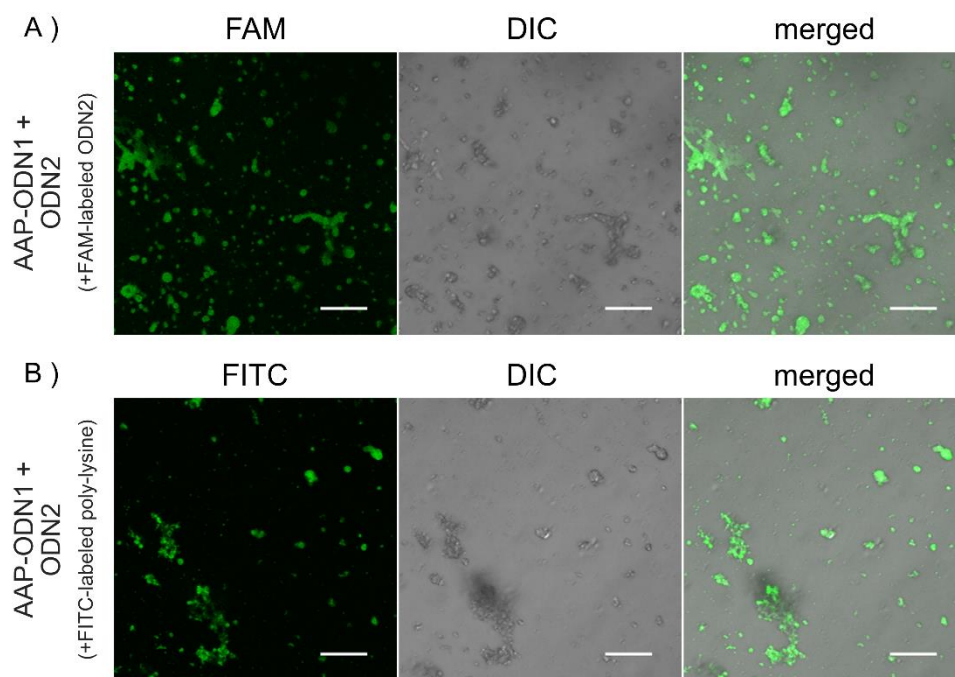
Fig S3. Fluorescence images of microcompartments of (A) 0.25 mM of AAP-ODN1, 0.2 mM of ODN2, 0.05 mM of FAM-labeled ODN2 and 5.0 mM of pLys mixture and (B) 0.25 mM of AAP-ODN1, 0.25 mM of ODN2, 4.0 mM of pLys and 1.0 mM of FITC-labeled pLys mixture in aqueous buffer containing 100 mM of NaCl.
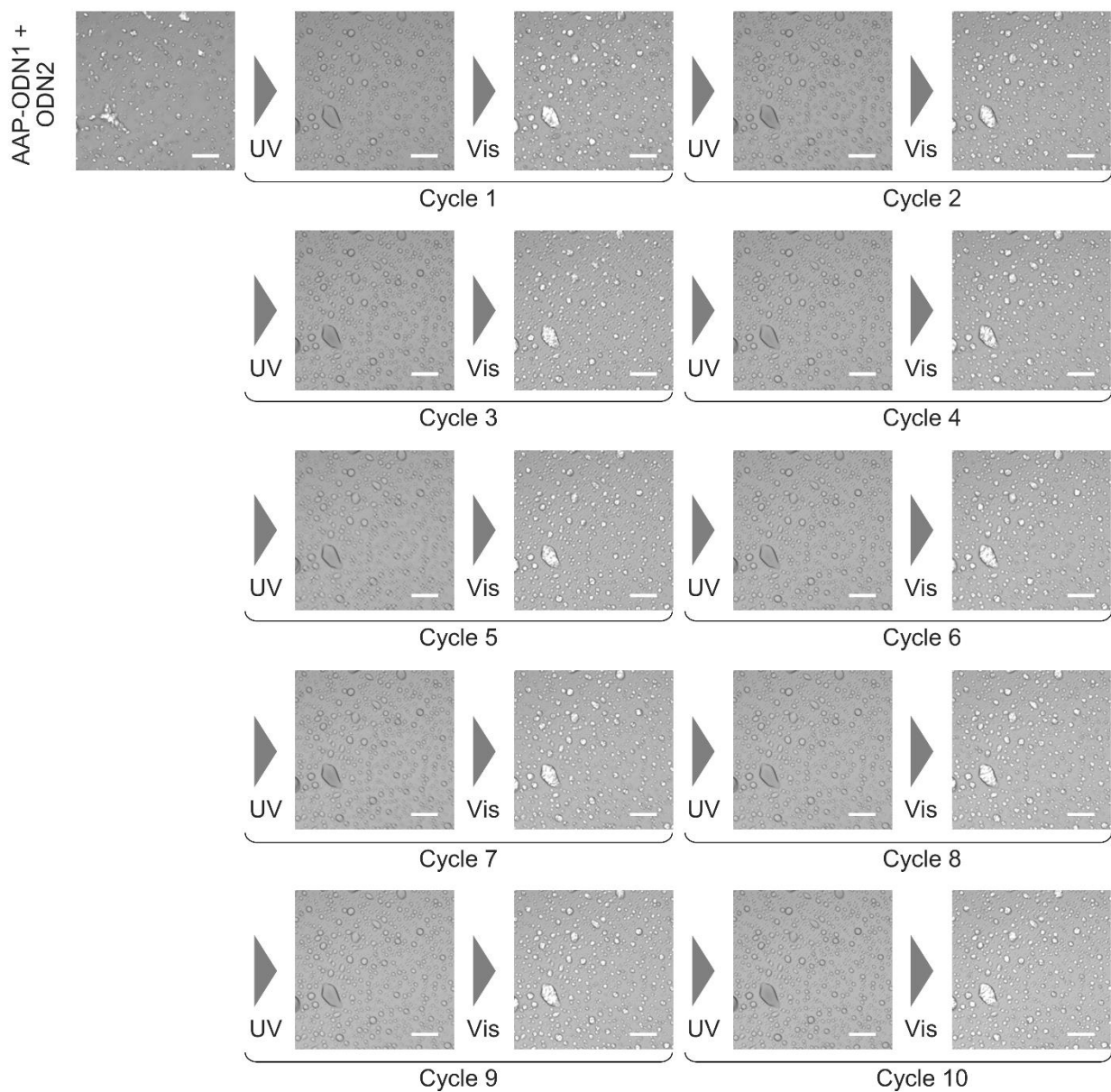
Fig S4. All polarized light microscopy images of microcompartments during repeated UV (340-390 nm) and visible light (530-550 nm) irradiation containing AAP-ODN1/ODN2 related to Fig. 3A. Scale bars are 20 μm.
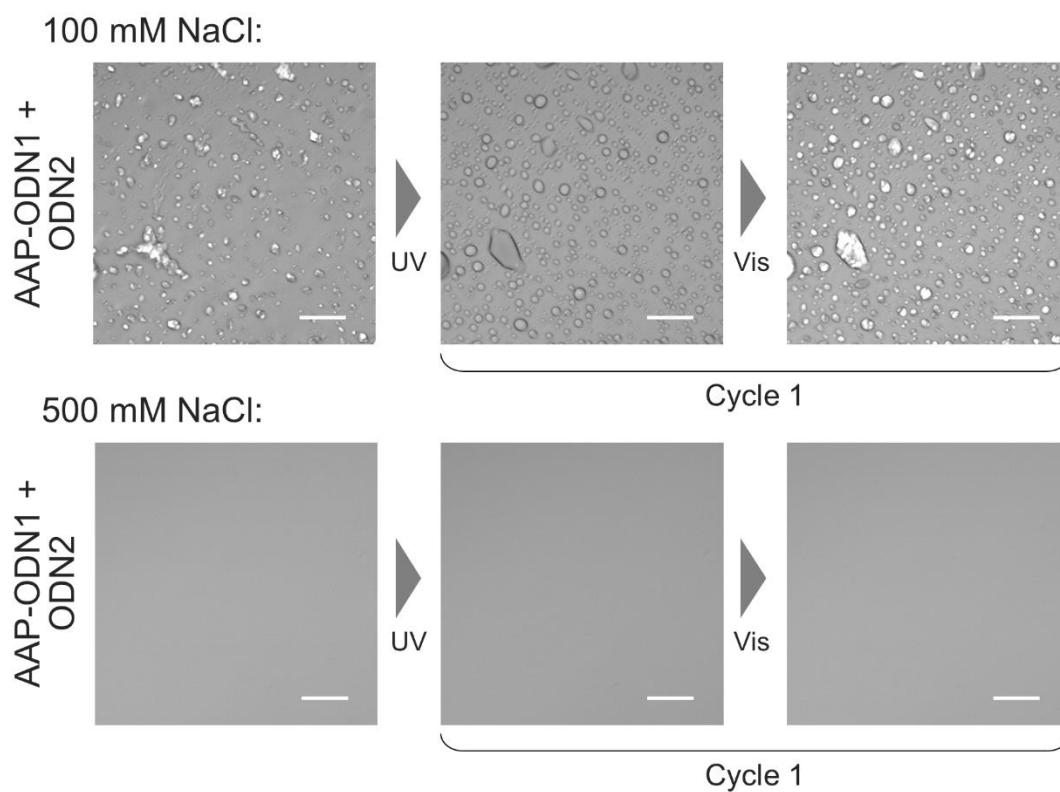
Fig S5. Polarized light microscopy images of microcompartments of AAP-ODN1/ODN2 at 100 mM and 500 mM NaCl. The samples were irradiated with UV (340-390 nm) and visible light (530-550 nm). Scale bars are 20 μm.

Associated reference

(1) Adam, V.; Prusty, D. K.; Centola, M.; Škugor, M.; Hannam, J. S.; Valero, J.; Klöckner, B.; Famulok, M. *Chem. Eur. J.* **2018**, *24*, 1062-1066.